

 Open access • Posted Content • DOI:10.1101/2021.08.04.455028

## **ComF is a key mediator in single-stranded DNA transport and handling during natural transformation** — [Source link](#)

Prashant P. Damke, Louisa Celma, Sumedha M. Kondekar, Anne Marie Di Guilmi ...+9 more authors

**Published on:** 06 Aug 2021 - [bioRxiv](#) (Cold Spring Harbor Laboratory)

**Topics:** [DNA transport](#) and [DNA](#)

Related papers:

- [The role of E. coli single-stranded DNA binding protein in DNA metabolism](#)
- [Origin Remodeling and Opening in Bacteria Rely on Distinct Assembly States of the DnaA Initiator](#)
- [New insights in the  \$\phi\$ 29 terminal protein DNA-binding and host nucleoid localization functions.](#)
- [Mediators of Homologous DNA Pairing](#)
- [Cellular location and activity of Escherichia coli RecG proteins shed light on the function of its structurally unresolved C-terminus](#)

Share this paper:    

View more about this paper here: <https://typeset.io/papers/comf-is-a-key-mediator-in-single-stranded-dna-transport-and-3maa8uvavp>

1  
2  
3  
4  
5  
6  
7  
8  
9  
10  
11  
12  
13  
14  
15  
16  
17  
18  
19  
20  
21  
22  
23  
24  
25  
26  
27  
28  
29  
30  
31  
32

## **ComF is a key mediator in single-stranded DNA transport and handling during natural transformation**

Prashant P. Damke<sup>1,2†</sup>, Louisa Celma<sup>3†</sup>, Sumedha Kondekar<sup>1,2</sup>, Anne Marie Di Guilmi<sup>1,2</sup>,  
Stéphanie Marsin<sup>3</sup>, Jordane Dépagne<sup>4</sup>, Xavier Veaute<sup>4</sup>, Pierre Legrand<sup>5</sup>, Hélène Walbott<sup>3</sup>,  
Julien Vercruyssen<sup>3</sup>, Raphaël Guérois<sup>3</sup>, Sophie Quevillon-Cheruel<sup>3\*</sup> and J. Pablo Radicella<sup>1,2\*</sup>

<sup>1</sup>. Université Paris-Saclay, CEA, Institut de Biologie François Jacob, Stabilité Génétique Cellules Souches et Radiations, F-92260 Fontenay aux Roses, France

<sup>2</sup>. Université de Paris, CEA, Institut de Biologie François Jacob, Stabilité Génétique Cellules Souches et Radiations, F-92260 Fontenay aux Roses, France

<sup>3</sup>. Université Paris-Saclay, CEA, CNRS, Institute for Integrative Biology of the Cell (I2BC), F-91198 Gif-sur-Yvette, France.

<sup>4</sup>. Université Paris-Saclay and Université de Paris, CEA, INSERM, Institut de Biologie François Jacob, Stabilité Génétique Cellules Souches et Radiations, F-92260 Fontenay aux Roses, France

<sup>5</sup>. Synchrotron SOLEIL, L'Orme des Merisiers, F-91192 Gif-sur-Yvette, France.

\* Corresponding authors : SQC, [sophie.quevillon-cheruel@i2bc.paris-saclay.fr](mailto:sophie.quevillon-cheruel@i2bc.paris-saclay.fr); JPR, [pablo.radicella@cea.fr](mailto:pablo.radicella@cea.fr)

† These authors contributed equally to this work

33 **ABSTRACT**

34

35 Natural transformation plays a major role in the spreading of antibiotic resistances and  
36 virulence factors. Whilst bacterial species display specificities in the molecular machineries  
37 allowing transforming DNA capture and integration into their genome, the ComF(C) protein is  
38 essential for natural transformation in all Gram- positive and - negative species studied.  
39 Despite this, its role remains largely unknown. Here, we show that *Helicobacter pylori* ComF  
40 is not only involved in DNA transport through the cell membrane, but it also required for the  
41 handling of the ssDNA once it is delivered into the cytoplasm. ComF crystal structure revealed  
42 the presence of a zinc-finger motif and a putative phosphoribosyl transferase domain, both  
43 necessary for its *in vivo* activity. ComF is a membrane-associated protein with affinity for  
44 single-stranded DNA. Collectively, our results suggest that ComF provides the link between  
45 the transport of the transforming DNA into the cytoplasm and its handling by the  
46 recombination machinery.

47

48

49

50

51

52

53

## 54 **Introduction**

55  
56 Bacterial populations display an amazing capacity to adapt to changes in their environment.  
57 In pathogens, this is reflected in the generation of variants able to colonise new hosts, the  
58 propagation of virulence factors or the acquisition antibiotics resistance. A key mechanism in  
59 the propagation of those traits is horizontal gene transfer (HGT). There are three major  
60 mechanisms of HGT in bacteria: conjugation, phage transduction and natural transformation  
61 (NT). Although NT has been documented in at least 80 bacterial species <sup>1</sup>, many aspects of the  
62 underlying mechanisms and players remain to be unveiled. Unlike the other pathways of HGT,  
63 NT only requires proteins coded by the recipient cell. It relies on the presence in naturally  
64 competent bacteria of a sophisticated apparatus capable of capturing DNA present in the  
65 environment and integrating it into their chromosome <sup>2</sup>.

66 In both gram-positive and -negative species, NT can be divided in four distinct steps <sup>2</sup>.  
67 It is initiated by the capture of exogenous double-stranded DNA (dsDNA) molecule at the  
68 surface of the cell where it binds to macromolecular complexes. During the uptake step,  
69 dsDNA is imported from the surface and into the periplasm (defined here as the  
70 compartments between the outer and inner membranes in gram-negative bacteria and  
71 between the cell wall and the membrane in gram-positive bacteria <sup>2</sup>). In the periplasm, the  
72 incoming DNA is directed to the inner cell membrane for its transport into the cytoplasm as  
73 single-stranded DNA (ssDNA). There, it is handled to the recombination machinery leading  
74 eventually to its incorporation into the chromosome, the last step of the process.

75 At each step of NT specialised proteins are required. Some of them are common to  
76 most species studied, but others are species-specific. While type IV pseudo-pili components  
77 have been shown to mediate the binding of the DNA to the cell surface in *Streptococcus*  
78 *pneumoniae* <sup>3</sup>, this observation cannot be generalised to all competent bacteria. In *Bacillus*  
79 *subtilis*, wall teichoic acids, but not the pseudo-pilus, are involved in the initial binding of the  
80 DNA <sup>4,5</sup>. Actually, in most cases the molecules responsible for DNA capture are still  
81 unidentified. *Helicobacter pylori*, a species characterised for its high capacity for NT, does not  
82 harbour genes coding for type IV (pseudo-)pili. As for the uptake step, in nearly all the  
83 naturally transformable bacteria it is mediated by a type IV pseudo-pilus <sup>2,6</sup>, with the exception  
84 of *H. pylori* that uses a type IV secretion system to pull the DNA into the periplasm <sup>7-9</sup>. To  
85 complete this step, the conserved DNA receptor ComEA, a periplasmic or membrane-

86 associated protein in gram-negative or gram-positive bacteria, respectively, is required. Here  
87 again, *H. pylori* constitutes an exception, since a unique protein, ComH, takes this role <sup>10</sup>. The  
88 transport step is carried out by the membrane channel ComEC <sup>6,9,11–13</sup>. ComEC is present and  
89 required for NT in all naturally transformable bacteria. Finally, the handing of the incoming  
90 DNA to the recombination machinery requires DprA <sup>14</sup>, another transformation-specific  
91 protein with orthologues in all naturally transformable species.

92 Other proteins essential for NT have been identified by genetics approaches, but their  
93 role is still unknown. One of them, ComF(C), is present in all naturally competent bacteria. The  
94 requirement of this protein for transformation was discovered almost 30 years ago <sup>15,16</sup>. The  
95 *B. subtilis* ComF locus consists of an operon harbouring three open reading frames coding for  
96 the proteins ComFA, ComFB and ComFC. All three are required for competence <sup>16,17</sup>. ComFA,  
97 which appears to be present in all naturally transformable Gram-positive bacteria but has not  
98 been identified in Gram-negative species, is a DNA-dependent ATPase <sup>18–20</sup>. A regulatory  
99 function has been proposed for ComFB <sup>17</sup>. In the case of ComFC, its function remains unknown  
100 despite being the only one of the three for which orthologues have been identified and  
101 described as essential for competence in all naturally transformable species studied.

102 Here, we characterised the ComF(C), herein ComF, from *H. pylori* and investigated its  
103 role in NT. Through the determination of its 3D structure we found that ComF harbours  
104 phosphoribosyl transferase (PRT) and Zn-finger domains, both essential for transformation.  
105 We show that in the absence of ComF, not only the transport of the transforming DNA (tDNA)  
106 into the cytoplasm is blocked but also its integration into the bacterial chromosome is  
107 impaired when the DNA is directly delivered to the cytoplasm. These phenotypes, together  
108 with the observations of ComF association with the inner cell membrane and its capacity to  
109 bind ssDNA suggest a model in which ComF role provides a link between the transport and  
110 recombination steps during NT.

111

## 112 Results and discussion

113

114 **ComF participates in DNA transport through the inner membrane.** Despite the critical role of  
115 natural transformation in bacterial evolution and in the propagation of virulence and  
116 antibiotic resistances, many aspects of the transforming DNA uptake and processing remain  
117 poorly understood. A notorious example is the role of the ComF protein, which, while its gene  
118 was identified almost 30 years ago as essential for competence<sup>15,16</sup> and conserved in all  
119 naturally transformable species studied so far, remains unknown. A transposon mutagenesis  
120 screen originally identified *hp1473 (comF)*, a *comFC* orthologue, as a gene essential for natural  
121 transformation in *H. pylori*<sup>21</sup>. In the present study we undertook the characterisation of this  
122 protein and its function by a combination of approaches to (i) define the step(s) at which the  
123 protein acts during NT, (ii) determine its 3D structure and (iii) analyse its biochemical  
124 properties.

125 To confirm the effect of *comF* inactivation on *H. pylori* NT, a *hp1473* null mutant was  
126 generated by insertion of a non-polar cassette and NT frequencies were determined using  
127 genomic DNA from a streptomycin resistant strain as transforming DNA. The absence of ComF  
128 led to almost a four log decrease in the transformation efficiency when compared to the wild-  
129 type strain (Fig. 1a). This phenotype, although less severe than that induced by inactivation of  
130 *comB*, *comEC* or *recA*, was similar to that observed for  $\Delta comH$  and  $\Delta dprA$  strains. Wild-type  
131 levels of transformation were restored by the re-expression of *comF* gene introduced with its  
132 own promoter at the *rdxA* locus (Fig. 1b), ruling out polar effects of the deletion.

133 We then sought to define at which stage(s) during the transformation process ComF is  
134 required. Deletion of *comF* did not affect the uptake step as illustrated by the presence of  
135 transforming DNA foci (Fig. 2a and b). Consistently with the cytoplasmic localisation of ComF  
136 and the two-steps model for DNA uptake<sup>9,22</sup>, the wild-type levels of DNA foci in  $\Delta comF$  strains  
137 indicated that ComF is not required for the exogenous DNA capture and uptake into the  
138 periplasm. The same conclusion was reached by monitoring by PCR the presence of tDNA in  
139  $\Delta comF$  mutant strains of *V. cholerae*<sup>6</sup>. However, when the persistence of the foci was  
140 monitored, we observed that in the  $\Delta comF$  strain foci are detected for longer times than in  
141 the wild type (Fig. 2b and c), similar to what was observed in a *comEC* mutant<sup>12</sup>. This  
142 suggested that ComF is needed for an efficient transport of the incoming DNA through the  
143 inner membrane. Consistently, when the kinetics of fluorescent DNA internalisation were

144 followed in living bacteria <sup>12</sup>, we observed that in the  $\Delta comF$  mutant, as it is the case in the  
145  $\Delta comEC$  one, the transforming DNA could not be detected as entering into the cytoplasm (Fig.  
146 [2d and Supplementary Movies 1-3](#)). These observations are very similar to those described in  
147  $\Delta comEC$  strains <sup>9,12</sup>, suggesting that ComEC and ComF act at the same NT step to mediate DNA  
148 transport across the inner membrane. Taken together, these results indicate that ComF  
149 participates in the passage of the transforming DNA into the cytosol.

150

151 **ComF is associated with the inner membrane.** A role of ComF in the tDNA translocation from  
152 the periplasm to the cytoplasm supposes a connection of the protein with the membrane. To  
153 explore such a possibility, we developed an antibody against ComF. Initially we were not able  
154 to detect the protein by immunoblot with this antibody, but by skipping the boiling step, a  
155 specific, albeit weak, signal was detectable in the wild-type strain extract ([Supplementary](#)  
156 [Figure 1](#)). We then fractionated the extracts into soluble and membrane fractions and we  
157 observed that ComF was associated with the membrane compartment (Fig. [3a](#)). Further  
158 fractionation showed that ComF co-purified with the inner membrane fraction (Fig. [3b](#)). To  
159 obtain a better signal, ComF fused to a FLAG tag (ComF-FLAG) was ectopically expressed from  
160 the *ureA* promoter. ComF-FLAG complementation of the *comF* deletion was less efficient, but  
161 could still support high levels of transformation (Fig. [1b](#)). ComF-FLAG was also present in the  
162 membrane fraction, although it could also be found in the soluble fraction probably due to its  
163 overexpression (Fig. [3c](#)).

164 The association of ComF with the membrane is consistent with the role of the protein  
165 facilitating the transport of the exogenous DNA through the inner cell membrane. The link to  
166 the membrane could be direct or mediated by either another protein or the incoming DNA. A  
167 candidate for coupling ComF to the membrane in Gram-positive bacteria could be ComFA. In  
168 *B. subtilis* ComFA was shown to be a membrane protein <sup>19</sup>. Furthermore, it was shown that its  
169 *S. pneumoniae* orthologue interacts with ComF(C) <sup>18</sup>. However, no orthologue of ComFA has  
170 been so far found in Gram-negative naturally transformable bacteria where ComF could  
171 interact with a functional, but yet to be identified, homologue of ComFA. Alternatively, ComF  
172 targeting to the membrane could be mediated by a completely unrelated protein. Finally,  
173 although unlikely in view of the lack of a membrane anchoring domain, ComF could be itself  
174 binding to the periphery of membranes.

175

176 **ComF is required for tDNA handling within the cytoplasm.** While the experiments described  
177 above demonstrated a role of ComF in the internalisation of the transforming DNA, they do  
178 not rule out its involvement in downstream steps of the natural transformation process. In  
179 order to test this possibility, the internalisation step, impaired in the  $\Delta comF$  mutant, needs to  
180 be bypassed. The transforming ssDNA was therefore delivered to the cytoplasm by  
181 electroporation. While ssDNA is a poor substrate for NT<sup>23</sup>, electroporation with a 75-mer  
182 ssDNA carrying a streptomycin resistance marker allowed transformation of mutants deficient  
183 in the uptake ( $\Delta comB2$ ) and internalisation ( $\Delta comEC$ ) steps<sup>10</sup>. However, after electroporatin  
184 with the same ssDNA, either much less or no streptomycin resistant transformants was  
185 observed for mutants affecting the homologous recombination process ( $\Delta dprA$ ,  $\Delta recA$ ) (Fig.  
186 4a). When a  $\Delta comF$  mutant was electroporated with the same ssDNA, the level of  
187 streptomycin resistant recombinants was similar to that obtained with a  $\Delta dprA$  strain. Similar  
188 results were obtained with a longer substrate (139-mer also carrying the mutation conferring  
189 streptomycin resistance) (Supplementary Figure 2). The reduced efficiency of a  $\Delta comF$  mutant  
190 in transformation by electroporation with single-stranded DNA suggests that ComF is involved  
191 in NT steps downstream of the transport through the inner membrane.

192 To further explore this role of ComF in the handling of the tDNA in the cytoplasm, we  
193 purified ComF and analysed its capacity to bind DNA by electrophoretic mobility shift assays  
194 (EMSA). ComF formed discrete nucleoprotein complexes with a 62-mer single-stranded DNA  
195 (ssDNA) in a concentration-dependent manner while no binding to the corresponding dsDNA  
196 was detectable (Fig. 4b). ComF bound single-stranded oligonucleotides with relatively high  
197 affinity (half-maximal binding concentration of 300 nM). This marked preference for ssDNA is  
198 consistent with the fact that during NT the incoming DNA enters the cytoplasm as ssDNA<sup>24</sup>.

199 The failure to bypass the transformation defect of mutant  $\Delta comF$  by electroporation  
200 with ssDNA together with the capacity of ComF to bind ssDNA, indicate that ComF is likely to  
201 be implicated in the steps leading to the formation of the recombination substrate within the  
202 cytoplasm. ComF could, together with DprA and RecA<sup>25</sup>, participate in the protection of the  
203 incoming DNA from degradation. Interestingly, ComF from *Campilobacter jejuni* and ComF(C)  
204 from *S. pneumoniae*, both required for natural transformation<sup>18,26</sup>, interact with DprA<sup>18,27</sup>.  
205 Since DprA plays a critical role in the loading of the recombinase to the transforming DNA<sup>14</sup>,  
206 it is tempting to speculate that ComF binds the tDNA emerging from ComEC into the



207 cytoplasm and targets it to DprA to protect it from degradation and allow further processing  
208 by the recombination machinery.

209

210 **ComF harbours zinc-finger and PRT domains.** Despite its conservation amongst naturally  
211 competent bacteria ([Supplementary Figure 3](#)), no structural data on ComF(C) proteins is  
212 available. The determination of its 3D structure has been elusive. After unsuccessful  
213 crystallisation attempts with the isolated protein we generated a gene fusion between the  
214 full-length *comF* gene and an artificial  $\alpha$ Rep binder coding sequence selected from a highly  
215 diverse library of artificial repeat proteins based on thermostable HEAT-like repeats in order  
216 to help cristallisation <sup>28,29</sup>. Since structural homology predictions using HHpred  
217 (<http://toolkit.tuebingen.mpg.de/hhpred/>)<sup>30</sup> suggested that the C-terminal domain of ComF  
218 (residues 53 to 188) harbours a putative nucleoside binding site characteristic of  
219 phosphoribosyl transferases (PRTases) belonging to the PRT family (PurF, PDB number 6CZF-  
220 A, probability 99.15%), crystals were grown in the presence of 5-phospho- $\alpha$ -D-ribose 1-  
221 pyrophosphate (PRPP). Diffracting crystals were obtained with the purified fusion protein and  
222 the 3D structure of full-length ComF in complex with PRPP was solved at 2.56 Å resolution  
223 ([Table 1](#), Materials and Methods) <sup>31</sup>. The fusion ( $\alpha$ Rep: residues 1–229, linker: residues 230–  
224 236, ComF: residues 237–427) is present in four copies in the asymmetric unit, organised in  
225 two domain-swapped dimers: the  $\alpha$ Rep of one fusion covers the ComF of the other one ([Fig.](#)  
226 [5a](#)). The 3D structure obtained confirmed the presence of two predicted distinct domains in  
227 ComF.

228 The presence of the  $\alpha$ Rep impeded to conclude from the crystal structure on the  
229 possibility of ComF adopting higher order quaternary structures. Most PRT proteins form  
230 dimers <sup>32</sup>. This, together with the dimers described for the *S. pneumoniae* ComFC protein <sup>18</sup>,  
231 prompted us to explore by bacterial two hybrid assays (BacTH) whether the *H. pylori*  
232 orthologue could also interact with itself. This was indeed the case ([Fig. 5b](#)). To better define  
233 the interaction mode, BacTH assays using the separate CTD (residues 26 – 191) and NTD  
234 (residues 1 – 25) domains were performed. While no signal above background was obtained  
235 when the individual domains were tested for the formation of homodimers, a strong  
236 interaction between the PRT and the Zn-finger domains was revealed, suggesting that  
237 HpComF could form head to tail dimers ([Fig. 5b](#)).

238

239 **The zinc-finger domain is required for ComF function.** The small NTD of ComF (residues M1–  
240 D21), which is part of a larger domain corresponding to the additional and variable “hood”  
241 domain of the PRTase family<sup>32</sup>, is a 4-Cys Zn-finger (in grey in [Fig. 5c](#) and [Supplementary Figure](#)  
242 [4a](#)). The Zn-finger is connected by a five amino acid linker to the rest of the hood domain  
243 (residues L22–T54), structured into a small sheet of two  $\beta$  strands followed by a kinked  $\alpha$  helix.  
244 A  $Zn^{2+}$  ion is liganded into the protein via the four cysteine residues (C3, C6, C15 and C18 in  
245 pink in [Supplementary Figure 4a](#)) which are highly conserved within the ComF(C) family  
246 ([Supplementary Figure 3](#)).

247 To explore the role of the zinc-finger, we expressed from either the *rdxA* or the *ureA*  
248 loci a ComF version in which cysteines 15 and 18 were replaced by serine (ComF-C15S,C18S),  
249 and tested its capacity to complement the transformation phenotype of a  $\Delta comF$  strain.  
250 Unlike the wild-type ComF, the mutant protein could not restore natural transformation ([Fig.](#)  
251 [1b](#)). Furthermore, mutation of the two cysteines hindered the integration into the bacterial  
252 chromosome of a ssDNA delivered by electroporation into the cytosol ([Fig. 4a](#)). Zinc-finger  
253 domains are most often found in proteins known to bind DNA or RNA<sup>33</sup>. In particular, 4-Cys  
254 zinc-fingers are present in ribosomal proteins or in enzymes involved in DNA replication,  
255 recombination and transcription<sup>34,35</sup>. Unfortunately, attempts to purify ComF versions either  
256 mutated in cysteines 15 and 18 or deleted of the zinc-finger domain were unsuccessful,  
257 preventing further exploration of its function at the biochemical level. There are, however,  
258 several examples of zinc-finger domains that do not participate in nucleic acid binding, but are  
259 involved in protein-protein interactions<sup>36,37</sup>. Interestingly, this is the case for RadA, a DNA  
260 helicase implicated in NT of Gram-positive bacteria. While RadA mutated in its 4-Cys domain  
261 is still able to bind DNA and to carry out its ATPase and helicase activities, it cannot interact  
262 with RecA, thus limiting its D-loop unwinding capacity<sup>38</sup>.

263 The closest structural homologue of the ComF zinc-finger is the zinc-finger domain of  
264 RecR, a recombination protein (RMSD of 0.8 Å for 22 aligned residues, PDB number 4O6O<sup>39</sup>  
265 or PDB number 5Z2V<sup>40</sup>). While the role of the RecR zinc-finger remains to be determined<sup>41,42</sup>,  
266 it has been suggested that it has a structural role in protein folding<sup>42</sup>. Supporting this  
267 possibility, as in our case, the authors were unable to produce soluble forms of *E. coli* or *H.*  
268 *pylori* RecR mutated in its zinc-finger cysteines. While it is tempting to speculate that ComF  
269 zinc-finger is involved in the binding of the transforming DNA, we cannot rule out a role of this

270 domain in the interaction of the protein with other NT partners. Further studies are required  
271 to define its precise role.

272

273 **The PRPP binding domain is necessary for ComF function.** The ComF CTD (residues L55–  
274 D190, the last E191 is not defined in the electron density) shares the common core of the  
275 amidophosphoribosyl transferase type 1 fold (RMSD between 2.6 and 3 Å for 100 to 130  
276 aligned residues, PDB number 5ZGO<sup>43</sup> as an example). A central parallel β sheet characteristic  
277 of the PRTase core domains is present (β strands <sup>183</sup>AIA<sup>185</sup>, <sup>153</sup>YFLLD<sup>157</sup>, <sup>85</sup>LYGIA<sup>89</sup> and <sup>113</sup>LKP<sup>115</sup>,  
278 in yellow in Fig. 5c), extended by the two β strands of the NTD (<sup>27</sup>KVRVL<sup>31</sup> and <sup>34</sup>VSVYS<sup>38</sup>, in  
279 grey in Fig. 5c). The three Mg•PRPP-binding loops of the family are present, providing a large  
280 hydrogen bonds network with the PRPP (in green in Fig. 5c and Supplementary Figures 3 and  
281 4b). An electron density that can correspond to an Mg<sup>2+</sup> ion is present close to the PRPP. The  
282 “PRPP loop” carries the canonical <sup>157</sup>DDIITGTTL<sup>166</sup> active site signature allowing the binding  
283 of the ribose-5-phosphate group of the PRPP (Supplementary Figures 3 and 4b). The most  
284 variable “PPi loop” (A<sup>89</sup> to H<sup>100</sup>) allowing the binding of the PPi group of the PRPP is slightly  
285 longer than the standard four amino acids loops. The “flexible loop” (L<sup>120</sup> to T<sup>144</sup>) closes the  
286 pocket of the binding site occupied in our structure by the PRPP (red sticks in Fig. 5c). The  
287 presence of all three loops (Supplementary Figures 3) is considered the signature of the PRT  
288 family<sup>32</sup>.

289 The PRPP-binding domain, present in a large variety of proteins, is known to bind small  
290 molecules such as nucleotides or NMPs<sup>32,44</sup>. We performed differential scanning  
291 fluorimetry/thermal shift assays to detect interactions of purified *H. pylori* His<sub>6</sub>-ComF with  
292 various potential ligands. Fig. 6a shows that the wild-type protein exhibited a T<sub>m</sub> of around  
293 46°C. In the presence of AMP the fluorescence maxima observed for the wild-type protein was  
294 shifted by +9°C, suggesting the stabilisation of the protein through binding of the nucleotide.  
295 Albeit to a lesser extent, ADP addition to ComF also resulted in an increase in melting  
296 temperature (Supplementary Table 1). No effect was observed with the triphosphate  
297 nucleotide. To confirm that the nucleotide binding was through the PRPP-binding domain, we  
298 purified a mutant version of the protein where the threonine165 present in the conserved  
299 <sup>155</sup>LLDDIITGTTL<sup>166</sup> motif was replaced by an alanine. ComF T165A had a melting temperature  
300 close to that of the wild-type, indicating that the amino acid replacement did not affect  
301 significantly the structure of the protein. However, the addition of the nucleotides had a very

302 modest effect on the thermal stability of the protein (Fig. 6b and Supplementary Table 1),  
303 confirming the role of the conserved threonine in ligand binding.

304 To assess the relevance of ComF nucleotide binding capacity in the function of the  
305 protein during NT, we expressed in a  $\Delta comF$  strain either ComF T165A from the *rdxA* locus  
306 and its own promoter or ComF-FLAG T165A at the *urea* locus. While ComF T165A restored to  
307 a certain extent the transformation capacity, the recombinant frequency was 43-fold lower  
308 than that obtained with the wild-type protein expressed in the same conditions (Fig. 1). In the  
309 case of the strain expressing ComF-FLAG T165A, the expression of the protein was unable to  
310 complement the transformation phenotype of the  $\Delta comF$  strain (Fig. 1b).

311 While the presence of a zinc-finger is consistent with an involvement of ComF in the  
312 handling of the transforming DNA, the fact that the protein belongs to the PRT family is  
313 surprising.<sup>32</sup> The majority of PRT proteins are enzymes that catalyse the displacement of  
314 pyrophosphate from PRPP by a nitrogen-containing nucleophile<sup>32</sup>. While there are other  
315 PRTases, those belonging to the PRT family are involved in nucleotide synthesis and salvage  
316 pathways. Our results (Supplementary Table 1) show that ComF PRT domain is capable of  
317 binding not only PRPP but also monophosphorylated nucleotides and, albeit with less affinity,  
318 nucleotide di-phosphates. The physiological ligand remains, however, to be determined.

319 In a few PRT proteins the PRTase capacity to bind PRPP or the nucleotide substrate has  
320 been co-opted for regulatory functions as described for two *Bacillus subtilis* regulators of gene  
321 expression. PurR binds to DNA operator sequences to repress the expression of purine genes.  
322 Binding of PRPP lowers its affinity for the DNA, triggering expression<sup>45</sup>. PyrR binds regulatory  
323 regions of pyrimidine genes transcripts attenuating their expression. Its affinity for the mRNA  
324 is regulated by UMP<sup>46</sup>. We thus asked if the T165A mutation affected ComF affinity for the  
325 ssDNA. Even though this substitution abolished the interaction with nucleotides  
326 (Supplementary Table 1) it did not significantly affect the binding of ssDNA (Fig. 6c and  
327 Supplementary Figure 5).

328 The experiments presented here do not allow to conclude on whether ComF PRT  
329 domain provides a PRTase activity or a regulatory function. An intriguing hypothesis is that  
330 the deoxyribomononucleotides released by the degradation of the non-transforming strand  
331<sup>47</sup> might regulate ComF capacity to bind DNA. Although ComF T165A is not affected in its DNA  
332 affinity (Fig. 6c), it is possible that binding to the wild-type protein of a so far unidentified  
333 nucleotide results in a reduced affinity for the transforming DNA. It is worth noting that the

334 T165A mutant, while completely impaired in nucleotide binding (Fig. 6b and Supplementary  
335 Table 1), can still partially rescue the transformation phenotype of a  $\Delta comF$  mutant (Figure  
336 1b), suggesting that nucleotide binding to ComF could provide a fine-tuning mechanism of the  
337 transformation process. Such a scenario would be consistent with the recently proposed  
338 hypothesis that ComF provides a link between transformation and metabolism<sup>48</sup>.

339

## 340 **Conclusion**

341

342 In this study, using *H. pylori* as a model, we sought to unveil the role of ComF, one of the most  
343 conserved proteins involved in horizontal gene transfer through NT. Despite the discovery of  
344 its essentiality for competence over 30 years ago, the understanding of where and how this  
345 protein participates in NT remained elusive. We showed here that ComF is required for at least  
346 two different steps in NT. First, ComF facilitates the transport of the tDNA through the cell  
347 membrane. Consistent with this finding we found that the protein localises to the inner  
348 membrane. Secondly, ComF, which we show has affinity for ssDNA, is involved in the handling  
349 of the DNA within the cytosol. We therefore propose that ComF provides a link between these  
350 two distinct steps during NT. Our structural studies demonstrated that ComF is composed of  
351 two conserved domains, both essential for its *in vivo* activity: a 4-Cys zinc-finger domain and  
352 a PRPP-binding domain. While several details of ComF mechanism of action remain to be  
353 elucidated, the data presented here shed light on the role of this protein critical for NT in all  
354 naturally competent bacteria.

355

## 356 **Methods**

357 ***H. pylori* cultures.** *H. pylori* strains are listed in Supplementary Table 2. Cultures were grown  
358 under microaerophilic conditions (5% O<sub>2</sub>, 10% CO<sub>2</sub>, using the MAC-MIC system from AES  
359 Chemunex) at 37 °C. Blood agar base medium (BAB) supplemented with 10% defibrillated  
360 horse blood (AES) was used for plate cultures. Liquid cultures were grown in brain heart  
361 infusion media (BHI) supplemented with 10% defibrillated and de-complemented fetal bovine  
362 serum (Invitrogen, Carlsbad, CA, USA) with constant shaking (180 rpm). Antibiotic mix  
363 containing polymyxin B (0.155 mg/ml), vancomycin (6.25 mg/ml), trimethoprim (3.125  
364 mg/ml), and amphotericin B (1.25 mg/ml) was added to both plate and liquid cultures.

365 Additional antibiotics were added as required: kanamycin (20 µg/ml), apramycin (12.5 µg/ml),  
366 and chloramphenicol (8 µg/ml) streptomycin (10 µg/ml) as required.

367

368 **Construction of gene variants in *H. pylori*.** All oligonucleotides and plasmids used in this work  
369 are listed in [Supplementary Tables 3 and 4](#). *H. pylori* 26695 gene sequences were obtained  
370 from the annotated complete genome sequence of 26695 deposited at  
371 <http://genolist.pasteur.fr/PyloriGene/>. Gene/locus specific primers (listed in [Supplementary](#)  
372 [Table 3](#)) were used to amplify region of interest by PCR, and fragments were joined together  
373 by either classical restriction-ligation method or using sequence- and ligation-independent  
374 cloning (SLIC). Different protein tags and mutations in the genes were introduced using SLIC  
375 or site directed mutagenesis, respectively. All the plasmids generated were verified by DNA  
376 sequencing (listed in [Supplementary Table 4](#)). The knock-out /Knock-in cassette were  
377 introduced into *H. pylori* by natural transformation. Their correct integration in *H. pylori*  
378 genome was confirmed by PCR using locus and gene specific primers. Verified strains (Table  
379 S2) were stored at -80 °C in BHI media supplemented with 12.5 % glycerol. The details of  
380 different constructions generated in this study are given below.

381

382 **Construction of *hp1473* null mutants in *H. pylori*.** To generate *hp1473* locus disrupted by a  
383 non-polar chloramphenicol cassette (*hp1473::Cm*), *hp1473* locus was amplified using gene  
384 specific primers (*hp1473F* and *hp1473R*) and ligated to blunt pJET1.2 vector to generate  
385 pJet1.2-*hp1473*. PCR fragments generated by amplification of this plasmid (using primers 1473  
386 inverse F and 1473 inverse R), and non-polar chloramphenicol (using primers KpnI-Cm-for and  
387 BamHI-Cm-rev) resistance cassette were digested using KpnI and BamHI and then ligated to  
388 generate the knockout cassette p978 (pJet1.2-*hp1473::Cm*).

389 To generate *hp1473* locus disrupted by a non-polar apramycin cassette  
390 (*hp1473::apramycin*), *hp1473* locus was amplified using primers Op853 and Op854 and ligated  
391 to pJET1.2 vector amplified using Op855-Op856 to generate pJet1.2- *hp1473*. The PCR  
392 fragments generated by amplification of pJet1.2-*hp1473* (using primers Op859 and Op860)  
393 and a non-polar apramycin resistance cassette (using primers Op857 and Op858) were ligated  
394 using SLIC to generate p1699.

395

396 **Ectopic expression of *hp1473* variants.** *hp1473* locus (+ 152 bp upstream sequence) was  
397 amplified using Op5 and Op6 and inserted in *rdXA::km* cassette present in the plasmid p1175  
398 (amplified using Op3 and Op4) using SLIC to generate plasmid p1176 . T165A and C15SC18S  
399 mutations in the *hp1473* coding region were introduced by PCR using mutagenic primers  
400 (op13+ Op14 and Op302 + Op303 respectively). The native *hp1473* locus was disrupted using  
401 p978. For expression using the *urea* promoter *hp1473* loci, wild-type or containing T165A or  
402 C15SC18S point mutations were amplified using Op611 and Op612 (containing the sequence  
403 for Flag tag) was ligated with p1088 (amplified using Op613 and Op614) containing the  
404 Promoter-UreA-Cm cassette using SLIC to generate p1672, p1674 and p1676 respectively.  
405 These plasmids were used to transform *H. pylori* followed by disruption of native *hp1473* locus  
406 was using p1699.

407

408 **Determination of transformation frequencies.** Natural transformation frequencies were  
409 determined as described <sup>49</sup>. Briefly, total chromosomal DNA (200 ng) from a streptomycin  
410 resistant but otherwise isogenic strain was incubated overnight with exponentially growing *H.*  
411 *pylori* cells (optical density of 4.0 at 600 nm), on solid medium. Next day, serial dilutions of *H.*  
412 *pylori* were spread on plates with and without streptomycin (10 µg/ml). Transformation  
413 frequencies after electroporation were determined as described <sup>10</sup>. Briefly, electro-  
414 competent cells were prepared by treating *H. pylori* cells (optical density of 10 OD/ml at 600  
415 nm) with ice-cold Glycerol 15 % + Sucrose 9 %. 50 µl of electro-competent cells mixed with 1  
416 µg of 139-mer or 75-mer-ssDNA ([Supplementary Table 3](#)) carrying A128G mutation in the  
417 *hp1197* gene were electroporated at 2.5 kV cm<sup>-1</sup> and 25 µF. The cells were mixed with 100 µl  
418 BHI, and 50 µl cells were spotted on BAB plates. Next day, serial dilutions of *H. pylori* cells  
419 were plated on plates with or without streptomycin (10 µg/ml). The transformation  
420 frequencies were calculated as the number of streptomycin resistance colonies per recipient  
421 colony-forming unit. *P* values were calculated using the Mann–Whitney *U* test on GraphPad  
422 Prism software.

423

424 **Fluorescence microscopy experiments.** Microscopy experiments were performed as  
425 described earlier <sup>10,12</sup>. Fluorescent dsDNA (408 bp) was prepared by amplification of *hp1197*  
426 locus from 26695 gDNA (100 ng) using primers 1197-5' and 1197-3' (0.5 µM each), 250 µM of  
427 dNTP mix, 5 Units of ExTaq enzyme (Takara) supplemented with 10 µM of ATTO-550-

428 aminoallyl-dUTP (Jena bioscience). PCR elongation was performed at 72 °C (2 min per kb) and  
429 the amplified products were purified by illustra GFX purification kit (GE Healthcare Little  
430 Chalfont, UK).

431 Exponentially growing *H. pylori* cells were incubated with fluorescent DNA (200 ng) for  
432 7 min at 37 °C, the unbound DNA was washed the bacteria were re-suspended in BHI, covered  
433 with low melting agarose (1.4 %) supplemented with 10 % fetal bovine serum and were  
434 observed under live conditions [gas mixture (10 % CO<sub>2</sub>, 3 % O<sub>2</sub>), humidity (90 %)] at 37 °C for  
435 3 h. Alternatively, the bacteria were fixed with 4 % formaldehyde (90 mins at 4 °C) followed  
436 by quenching with 100 mM Glycine. All the images were captured with 60X objective using  
437 inverted Nikon A1R confocal laser scanning microscope system. The images were processed  
438 and analyzed using NIS-element software (Nikon Corp., Tokyo, Japan) and ImageJ software.  
439 The percentage of bacteria with DNA foci was calculated as the number of bacteria with DNA  
440 foci over total number of bacteria counted in at least two independent biological replicates.  
441 To monitor the time dependent stability DNA foci, the total number of bacteria with DNA foci  
442 at t=15 mins were considered as 100%. The volumes of internalised DNA in GFP expressing  
443 bacteria were estimated by 3-D image analysis performed using Volocity software (Perkin  
444 Elmer, Waltham, USA).

445

446 **Subcellular fractionation.** Subcellular fractions of exponentially growing *H. pylori* were  
447 collected by differential centrifugation and detergent mediated solubilisation as described  
448 earlier<sup>10</sup>. Briefly, 100 ml cell pellet was re-suspended in buffer A (10 mM Tris-HCl, pH 7.5,  
449 1mM DTT, 1X protease inhibitor cocktail) followed by lysis by sonication. Total extracts were  
450 centrifuged 14,000 rpm for 15 minutes. The supernatant containing the soluble fraction was  
451 collected after ultracentrifugation at 45,000 rpm for 45 min of the total extract. The pellet  
452 containing the membrane fractions was re-suspended in buffer B (10 mM Tris-HCl, pH 7.5,  
453 1mM DTT, 1X protease inhibitor cocktail, 1% N-Lauroylsarcosine). The supernatant containing  
454 the inner membrane fractions were collected after ultracentrifugation at 45,000 rpm for 45  
455 min. The presence of the proteins in the various fractions was monitored by immunoblotting.

456

457 **Western blots.** The fractionation samples were resolved on a 15% SDS-PAGE, transferred on  
458 a nitrocellulose membrane. The membrane was blocked with 2% BSA prepared in PBST (1X  
459 PBS + 0.03% Tween 20). Blots were probed with either a mouse monoclonal anti-Flag antibody



460 (1: 5000 dilution, Sigma Aldrich), rabbit anti-MotB antibody (1: 2500 dilution) (kind gift from  
461 Dr. Ivo Boneca, Pasteur Institute) or rabbit anti-HpComF antibody from our laboratory  
462 collection. The blots were then probed with Advansta fluorescently labeled secondary  
463 antibodies IR700 and IR800 respectively. The imaging was done using Odyssey Clx imaging  
464 system.

465  
466 ***E. coli* cultures.** *Escherichia coli* strains used for cloning, protein overexpression and  
467 purification were cultured in Luria–Bertani (LB) broth, or LB agar plates supplemented with  
468 the required antibiotics [ampicillin (100 µg/ml), kanamycin (50 µg/ml), apramycin (50 µg/ml),  
469 or chloramphenicol (34 µg/ml)].

470  
471 **Protein samples preparation.** Cloning of *comF* (*Hp1473*) coding region was performed using  
472 genomic DNA from *H. pylori* strain 26695 as template for PCR. Six histidine codons were added  
473 at the 5' end during the PCR process. The fragment was inserted into the *NdeI-XhoI* sites of  
474 pET21a vector (Novagen). Site directed mutagenesis was performed using the resulting  
475 pET21:ComF-6His plasmid as a template and non-overlapping oligonucleotides  
476 phosphorylated in 5' (Eurofins), to construct the *HpComF*<sup>T165A</sup> mutant. The fusion of *comF* with  
477 an  $\alpha$ Rep protein (named B2), for its structural study, is described in <sup>31</sup>.

478 Expression of ComF or its mutant forms in BL21(DE3) Gold strain was performed in 800  
479 ml 2xYT o/n at 37°C after induction with 0.5 mM IPTG (Sigma). Cells were harvested by  
480 centrifugation, resuspended in buffer 500 mM NaCl, 20 mM Tris-HCl (pH 7.5), 5% glycerol for  
481 ComF-6His constructs, or in buffer 1 M NaCl, 100 mM Tris-HCl (pH 8), 100 µM TCEP for B2-  
482 ComF-6His (SeMet labelled according to the protocol described in <sup>50</sup> and stored at –20°C. Cell  
483 lysis was completed by sonication (probe-tip sonicator Branson). After centrifugation at  
484 20,000 g and 8°C for 30 min, the proteins were purified on a Ni-NTA column (Qiagen Inc.),  
485 eluted with imidazole. ComF-6His and B2-ComF-6His were then desalted up to 100 mM NaCl  
486 and loaded respectively onto a Heparin and a MonoQ column (Amersham Pharmacia Biotech)  
487 and eluted with a gradient of NaCl (from 100 mM to 1 M). The proteins were desalted up to  
488 200 mM NaCl and concentrated using Vivaspin 5,000 or 30,000 nominal molecular weight limit  
489 cut-off centrifugal concentrators (Sartorius), respectively, aliquoted, flash frozen in liquid  
490 nitrogen and stored at -80°C, or dialyzed in a 50% (vol/vol) glycerol buffer for storage at -20°C.

491

492 **Electrophoretic mobility shift assay.** DNA binding assays were performed by incubating  
493 indicated concentrations of proteins with fixed concentrations of Cy5 labelled DNA  
494 ([Supplementary Table 3](#)) in binding buffer (10 mM Tris-HCl pH 7.5, 50 mM KCl, 1 mM DTT, 0.1  
495  $\mu\text{g}/\mu\text{l}$  BSA) in cold room for 30 min. The nucleoprotein complexes were separated using native  
496 TBE-PAGE (6%). The gels were visualized by using Typhoon. The depletion in substrate DNA  
497 was quantified using ImageJ by considering DNA without protein as 100%.

498  
499 **Crystal structure determination.** SeMet modified B2-HpComF-6His (12.5 mg/ml) was  
500 incubated with PRPP (3 mM) and  $\text{MgCl}_2$  (5 mM) at 4°C. Crystals were grown in hanging drops  
501 by mixing the protein with reservoir solution in a 1:1 ratio. Crystals appeared after 5 days at  
502 4°C in 0.2 M Tri-potassium citrate + 18% PEG 3350. Glycerol cryo-protected crystals (two steps  
503 at 15 and 30%) were flash frozen in liquid nitrogen.

504 Diffraction data and refinement statistics are given in [Table 1](#). Crystallographic data  
505 were collected at the selenium peak wavelength on the PROXIMA-2A from Synchrotron SOLEIL  
506 (Saint-Aubin, France) and processed with XDS<sup>51</sup> through XDSME  
507 (<https://github.com/legrandp/xdsme>). Diffraction anisotropy was corrected using the  
508 STARANISO server (<http://staraniso.globalphasing.org>). The structure was solved by the SAD  
509 phasing method at 2.5 Å resolution using SHELX C/D<sup>52</sup> to locate the 12 heavy atom sites,  
510 PHASER<sup>53</sup> to determine the initial phases and PARROT<sup>54</sup> to improve the phases by density  
511 modification, through the CCP4 program suite<sup>55</sup>. The construction of the model was initiated  
512 using Buccaneer<sup>56</sup> and refined with the BUSTER using TLS and NCS restraints<sup>57</sup>. The model  
513 was corrected and completed using COOT<sup>58</sup>. The presence of a  $\text{Zn}^{2+}$  ion in the B2-HpComF  
514 structure was demonstrated by an energy scan performed on the crystals at the beamline  
515 (energy peak at 9.664 keV). Exploration of the 3D structures was performed using the  
516 following tools: Dali server<sup>59</sup>, I-TASSER<sup>60</sup> and SWISS-MODEL servers<sup>61</sup> and PyMOL Molecular  
517 Graphics System (<http://www.pymol.org>).

518  
519 **Bacterial Two-Hybrid assays.** The Bacterial Two-Hybrid test was used to probe the  
520 interactions between proteins<sup>62</sup>. The full-length ComF encoding sequence was fused to T18,  
521 at the C-terminal and N-terminal ends, T18-ComF (pUT18C vector) and ComF-T18 (pUT18  
522 vector), respectively. The same strategy has been used for ZnF and PRPP, the N-terminal and

523 C-terminal domains of ComF, respectively. Plasmids encoding T25-ComF, ComF-T25 and T25-  
524 PRPP were constructed using the pKT25 and pKNT25 vectors.

525 Plasmids encoding T18 and T25 fusion proteins were co-transformed in *E. coli* strain  
526 BTH101 and transformants were selected in Luria-Bertani agar plates containing kanamycin  
527 and ampicillin at 30°C. Colonies were then spotted on plates containing kanamycin, ampicillin,  
528 IPTG and X-gal, incubated at 30°C and stored at RT to follow the appearance and evolution of  
529 the blue colour.

530

531 **Differential Scanning Fluorimetry/Thermal shift assay.** Purified protein (10.5 µg) was  
532 incubated with different analytes in reaction buffer (20 mM Tris-Cl, pH 7.5, 200 mM NaCl, 5X  
533 Sypro Orange). The temperature of the reaction mixture was raised from 25 °C to 95 °C. Shift  
534 in the fluorescence due to binding of the Sypro-Orange dye as the hydrophobic patches of the  
535 protein were exposed due to denaturation of the protein was recorded. The fluorescence  
536 maxima observed was used to calculate the approximate melting temperature of the protein  
537 in native conditions and in presence of the analyte.

538

#### 539 **Data availability**

540 The atomic coordinates and structure factors of B2-HpComF have been deposited at the  
541 Brookhaven Protein Data Bank under the accession number 7POH.

542 All the other data are available in the main text or the supplementary materials.

543

#### 544 **REFERENCES**

- 545 1. Johnston, C., Martin, B., Fichant, G., Polard, P. & Claverys, J. P. Bacterial transformation:  
546 distribution, shared mechanisms and divergent control. *Nat Rev Microbiol* **12**, 181–196  
547 (2014).
- 548 2. Dubnau, D. & Blokesch, M. Mechanisms of DNA Uptake by Naturally Competent Bacteria.  
549 *Annual Review of Genetics* vol. 53 217–237 (2019).
- 550 3. Laurenceau, R. *et al.* A Type IV Pilus Mediates DNA Binding during Natural Transformation in  
551 *Streptococcus pneumoniae*. *PLoS Pathog* **9**, e1003473 (2013).
- 552 4. Briley, K. J. *et al.* The secretion ATPase ComGA is required for the binding and transport of  
553 transforming DNA. *Mol Microbiol* **81**, 818–830 (2011).
- 554 5. Mirouze, N., Ferret, C., Cornilleau, C. & Carballido-López, R. Antibiotic sensitivity reveals that  
555 wall teichoic acids mediate DNA binding during competence in *Bacillus subtilis*. *Nat. Commun.*  
556 **9**, 1–11 (2018).
- 557 6. Seitz, P. & Blokesch, M. DNA-uptake machinery of naturally competent *Vibrio cholerae*. *Proc.*  
558 *Natl. Acad. Sci. U. S. A.* **110**, 17987–17992 (2013).
- 559 7. Hofreuter, D., Odenbreit, S., Henke, G. & Haas, R. Natural competence for DNA

- 560 transformation in *Helicobacter pylori*: identification and genetic characterization of the comB  
561 locus. *Mol Microbiol* **28**, 1027–1038 (1998).
- 562 8. Karnholz, A. *et al.* Functional and topological characterization of novel components of the  
563 comB DNA transformation competence system in *Helicobacter pylori*. *J Bacteriol* **188**, 882–  
564 893 (2006).
- 565 9. Stingl, K., Muller, S., Scheidgen-Kleyboldt, G., Clausen, M. & Maier, B. Composite system  
566 mediates two-step DNA uptake into *Helicobacter pylori*. *Proc Natl Acad Sci U S A* **107**, 1184–  
567 1189 (2010).
- 568 10. Damke, P. P. *et al.* Identification of the periplasmic DNA receptor for natural transformation  
569 of *Helicobacter pylori*. *Nat. Commun.* **10**, 1–11 (2019).
- 570 11. Draskovic, I. & Dubnau, D. Biogenesis of a putative channel protein, ComEC, required for DNA  
571 uptake: membrane topology, oligomerization and formation of disulphide bonds. *Mol*  
572 *Microbiol* **55**, 881–896 (2005).
- 573 12. Corbinais, C., Mathieu, A., Kortulewski, T., Radicella, J. P. & Marsin, S. Following transforming  
574 DNA in *Helicobacter pylori* from uptake to expression. *Mol. Microbiol.* **101**, 1039–1053 (2016).
- 575 13. Pimentel, Z. T. & Zhang, Y. Evolution of the Natural Transformation Protein, ComEC, in  
576 Bacteria. *Front. Microbiol.* **9**, 2980 (2018).
- 577 14. Mortier-Barriere, I. *et al.* A key presynaptic role in transformation for a widespread bacterial  
578 protein: DprA conveys incoming ssDNA to RecA. *Cell* **130**, 824–836 (2007).
- 579 15. Larson, T. G. & Goodgal, S. H. Donor DNA processing is blocked by a mutation in the com101A  
580 locus of *Haemophilus influenzae*. *J Bacteriol* **174**, 3392–3394 (1992).
- 581 16. Londono-Vallejo, J. A. & Dubnau, D. comF, a *Bacillus subtilis* late competence locus, encodes a  
582 protein similar to ATP-dependent RNA/DNA helicases. *Mol Microbiol* **9**, 119–131 (1993).
- 583 17. Sysoeva, T. A. *et al.* Structural characterization of the late competence protein ComFB from  
584 *Bacillus subtilis*. *Biosci. Rep.* **35**, 183 (2015).
- 585 18. Diallo, A. *et al.* Bacterial transformation: ComFA is a DNA-dependent ATPase that forms  
586 complexes with ComFC and DprA. *Mol Microbiol* **105**, 741–754 (2017).
- 587 19. Londoño-Vallejo, J. A. & Dubnau, D. Membrane association and role in DNA uptake of the  
588 *Bacillus subtilis* PriA anaologue ComF1. *Mol. Microbiol.* **13**, 197–205 (1994).
- 589 20. Chilton, S. S., Falbel, T. G., Hromada, S. & Burton, B. M. A conserved metal binding motif in the  
590 *Bacillus subtilis* competence protein ComFA enhances transformation. *J. Bacteriol.* **199**,  
591 (2017).
- 592 21. Chang, K. C., Yeh, Y. C., Lin, T. L. & Wang, J. T. Identification of genes associated with natural  
593 competence in *Helicobacter pylori* by transposon shuttle random mutagenesis. *Biochem*  
594 *Biophys Res Commun* **288**, 961–968 (2001).
- 595 22. Kruger, N. J. & Stingl, K. Two steps away from novelty--principles of bacterial DNA uptake. *Mol*  
596 *Microbiol* **80**, 860–867 (2011).
- 597 23. Levine, S. M. *et al.* Plastic cells and populations: DNA substrate characteristics in *Helicobacter*  
598 *pylori* transformation define a flexible but conservative system for genomic variation. *FASEB J*  
599 **21**, 3458–3467 (2007).
- 600 24. Mejean, V. & Claverys, J. P. DNA processing during entry in transformation of *Streptococcus*  
601 *pneumoniae*. *J. Biol. Chem.* **268**, 5594–5599 (1993).
- 602 25. Bergé, M., Mortier-Barrière, I., Martin, B. & Claverys, J. P. Transformation of *Streptococcus*  
603 *pneumoniae* relies on DprA- and RecA-dependent protection of incoming DNA single strands.  
604 *Mol. Microbiol.* **50**, 527–536 (2003).
- 605 26. Wiesner, R. S., Hendrixson, D. R. & DiRita, V. J. Natural transformation of *Campylobacter jejuni*  
606 requires components of a type II secretion system. *J. Bacteriol.* **185**, 5408–5418 (2003).
- 607 27. Parrish, J. R. *et al.* A proteome-wide protein interaction map for *Campylobacter jejuni*.  
608 *Genome Biol.* **8**, (2007).
- 609 28. Guellouz, A. *et al.* Selection of Specific Protein Binders for Pre-Defined Targets from an  
610 Optimized Library of Artificial Helicoidal Repeat Proteins (alphaRep). *PLoS One* **8**, 71512  
611 (2013).

- 612 29. Valerio-Lepiniec, M. *et al.* The arep artificial repeat protein scaffold: A new tool for  
613 crystallization and live cell applications. *Biochem. Soc. Trans.* **43**, 819–824 (2015).
- 614 30. Zimmermann, L. *et al.* A Completely Reimplemented MPI Bioinformatics Toolkit with a New  
615 HHpred Server at its Core. *J. Mol. Biol.* **430**, 2237–2243 (2018).
- 616 31. Chevrel, A. *et al.* Alpha repeat proteins (αRep) as expression and crystallization helpers. *J.*  
617 *Struct. Biol.* **201**, 88–99 (2018).
- 618 32. Sinha, S. C. & Smith, J. L. The PRT protein family. *Current Opinion in Structural Biology* vol. 11  
619 733–739 (2001).
- 620 33. Pabo, C. O. & Sauer, R. T. Transcription factors: Structural families and principles of DNA  
621 recognition. *Annual Review of Biochemistry* vol. 61 1053–1095 (1992).
- 622 34. Leon, O. & Roth, M. Zinc fingers: DNA binding and protein-protein interactions. *Biol. Res.* **33**,  
623 21–30 (2000).
- 624 35. Laity, J. H., Lee, B. M. & Wright, P. E. Zinc finger proteins: New insights into structural and  
625 functional diversity. *Current Opinion in Structural Biology* vol. 11 39–46 (2001).
- 626 36. Crossley, M., Merika, M. & Orkin, S. H. Self-association of the erythroid transcription factor  
627 GATA-1 mediated by its zinc finger domains. *Mol. Cell. Biol.* **15**, 2448–2456 (1995).
- 628 37. Sun, L., Liu, A. & Georgopoulos, K. Zinc finger-mediated protein interactions modulate Ikaros  
629 activity, a molecular control of lymphocyte development. *EMBO J.* **15**, 5358–5369 (1996).
- 630 38. Marie, L. *et al.* Bacterial RadA is a DnaB-Type helicase interacting with RecA to promote  
631 bidirectional D-loop extension. *Nat. Commun.* **8**, (2017).
- 632 39. Tang, Q. *et al.* RecOR complex including RecR N-N dimer and RecO monomer displays a high  
633 affinity for ssDNA. *Nucleic Acids Res.* **40**, 11115–11125 (2012).
- 634 40. Che, S., Chen, Y., Liang, Y., Zhang, Q. & Bartlam, M. Crystal structure of RecR, a member of the  
635 RecFOR DNA-repair pathway, from *Pseudomonas aeruginosa* PAO1. *Acta Crystallogr. Sect. F*  
636 *Struct. Biol. Commun.* **74**, 222–230 (2018).
- 637 41. Ayora, S., Stiege, A. C. & Alonso, J. C. RecR is a zinc metalloprotein from *Bacillus subtilis* 168.  
638 *Mol. Microbiol.* **23**, 639–647 (1997).
- 639 42. Lee, B. *et al.* Ring-shaped architecture of RecR: Implications for its role in homologous  
640 recombinational DNA repair. *EMBO J.* **23**, 2029–2038 (2004).
- 641 43. Arco, J. Del *et al.* Structural and functional characterization of thermostable biocatalysts for  
642 the synthesis of 6-aminopurine nucleoside-5'-monophosphate analogues. *Bioresour. Technol.*  
643 **276**, 244–252 (2019).
- 644 44. Schramm, V. L. & Grubmeyer, C. Phosphoribosyltransferase Mechanisms and Roles in Nucleic  
645 Acid Metabolism. *Prog. Nucleic Acid Res. Mol. Biol.* **78**, 261–304 (2004).
- 646 45. Weng, M., Nagy, P. L. & Zalkin, H. Identification of the *Bacillus subtilis* pur operon repressor.  
647 *Proc. Natl. Acad. Sci. U. S. A.* **92**, 7455–7459 (1995).
- 648 46. Swtzer, R. L., Turner, R. J. & Lu, Y. Regulation of the *Bacillus subtilis* Pyrimidine Biosynthetic  
649 Operon by Transcriptional Attenuation: Control of Gene Expression by an mRNA-Binding  
650 Protein. *Prog. Nucleic Acid Res. Mol. Biol.* **62**, 329–348 (1998).
- 651 47. Dubnau, D. & Cirigliano, C. Fate of transforming DNA following uptake by competent *Bacillus*  
652 *subtilis*. IV. The endwise attachment and uptake of transforming DNA. *J Mol Biol* **64**, 31–46  
653 (1972).
- 654 48. De Santis, M., Hahn, J. & Dubnau, D. ComEB protein is dispensable for the transformation but  
655 must be translated for the optimal synthesis of comEC. *Mol. Microbiol.* 1–9 (2021)  
656 doi:10.1111/mmi.14690.
- 657 49. Damke, P. P., Dhanaraju, R., Marsin, S., Radicella, J. P. & Rao, D. N. The nuclease activities of  
658 both the Smr domain and an additional LDLK motif are required for an efficient anti-  
659 recombination function of *Helicobacter pylori* MutS2. *Mol. Microbiol.* **96**, 1240–1256 (2015).
- 660 50. Quevillon-Cheruel, S. *et al.* Cloning, production, and purification of proteins for a medium-  
661 scale structural genomics project. *Methods Mol Biol* **363**, 21–37 (2007).
- 662 51. Kabsch, W. XDS. *Acta Crystallogr. Sect. D Biol. Crystallogr.* **66**, 125–132 (2010).
- 663 52. Schneider, T. R. & Sheldrick, G. M. Substructure solution with SHELXD. *Acta Crystallogr. Sect.*

- 664 *D Biol. Crystallogr.* **58**, 1772–1779 (2002).
- 665 53. McCoy, A. J. *et al.* Phaser crystallographic software. *J. Appl. Crystallogr.* **40**, 658–674 (2007).
- 666 54. Cowtan, K. Recent developments in classical density modification. *Acta Crystallogr. Sect. D*
- 667 *Biol. Crystallogr.* **66**, 470–478 (2010).
- 668 55. Winn, M. D. *et al.* Overview of the CCP4 suite and current developments. *Acta*
- 669 *Crystallographica Section D: Biological Crystallography* vol. 67 235–242 (2011).
- 670 56. Cowtan, K. Fitting molecular fragments into electron density. in *Acta Crystallographica Section*
- 671 *D: Biological Crystallography* vol. 64 83–89 (International Union of Crystallography, 2007).
- 672 57. Smart, O. S. *et al.* Exploiting structure similarity in refinement: Automated NCS and target-
- 673 structure restraints in BUSTER. *Acta Crystallogr. Sect. D Biol. Crystallogr.* **68**, 368–380 (2012).
- 674 58. Emsley, P., Lohkamp, B., Scott, W. G. & Cowtan, K. Features and development of Coot. *Acta*
- 675 *Crystallogr. Sect. D Biol. Crystallogr.* **66**, 486–501 (2010).
- 676 59. Holm, L. & Rosenström, P. Dali server: Conservation mapping in 3D. *Nucleic Acids Res.* **38**,
- 677 W545–W549 (2010).
- 678 60. Zhang, Y. I-TASSER server for protein 3D structure prediction. *BMC Bioinformatics* **9**, (2008).
- 679 61. Arnold, K., Bordoli, L., Kopp, J. & Schwede, T. The SWISS-MODEL workspace: A web-based
- 680 environment for protein structure homology modelling. *Bioinformatics* **22**, 195–201 (2006).
- 681 62. Karimova, G., Pidoux, J., Ullmann, A. & Ladant, D. A bacterial two-hybrid system based on a
- 682 reconstituted signal transduction pathway. *Proc Natl Acad Sci U S A* **95**, 5752–5756 (1998).
- 683
- 684

685 **Figure Legends**

686 **Fig. 1: ComF is essential for genetic transformation of *H. pylori*.** (a) Natural transformation  
687 frequencies for indicated *H. pylori* strains. (b) Complementation of the  $\Delta comF$  strain. Natural  
688 transformation frequencies for indicated *H. pylori* strains were determined using isogenic  
689 streptomycin resistant total genomic DNA as donor. Bars correspond to the mean and  
690 standard deviation from at least three independent biological replicates. ns, not significant ( $P$   
691  $> 0.05$ );  $**P < 0.01$ ,  $***P < 0.001$  and  $****P < 0.0001$ .  $P$  values were calculated using the  
692 Mann–Whitney  $U$  test on GraphPad Prism software.

693

694 **Fig. 2: ComF supports translocation of tDNA across the cytoplasmic membrane.** (a)  
695 Percentage of cells with fluorescent DNA foci for indicated *H. pylori* strains. Bars correspond  
696 to the average and standard deviation from at least two independent biological experiments.  
697 (b) Time course of DNA foci for indicated *H. pylori* strains. Z maximum projections of merged  
698 images of ATTO-550 (red channel) and differential interference contrast (DIC) are presented.  
699 (c) Stability of DNA foci displayed by *H. pylori* strains. Data points correspond to the mean and  
700 standard deviation from at least two independent experiments except for the  $\Delta comEC$  strain.  
701 (d) Internalization kinetics of fluorescent DNA in indicated *H. pylori* strains. GFP expressing  
702 bacteria displaying fluorescent DNA foci were followed for 3 h by confocal microscopy in live  
703 conditions (Supplementary Movies 1-3). The mean  $\pm$ SEM volumes of DNA internalized were  
704 measured by 3D-analysis of individual bacterial cells for wild-type ( $n=26$ ),  $\Delta comEC$  ( $n=25$ ),  
705  $\Delta comF$  ( $n=148$ ) strains. At least two independent experiments were performed for each strain  
706 except for  $\Delta comEC$ .  $P$ -values calculated using Kruskal–Wallis statistics indicate that  $\Delta comEC$   
707 ( $p<0.0001$ ),  $\Delta dprA$  ( $p<0.0050$ ), and  $\Delta comF$  ( $p=0.0003$ ) curves are significantly different from  
708 the wild-type curve.

709

710 **Fig. 3: ComF is a membrane-associated protein.** (a) and (b) Localisation of ComF in wild-type  
711 *H. pylori* strain. (c) Localisation of overexpressed ComF-FLAG. The inner membrane protein  
712 MotB was used as marker for the fractionation experiments. T: total extract, S: soluble  
713 fraction, M: membrane. B: boiled samples, NB: not boiled samples.

714

715

716 **Fig. 4: ComF binds single-stranded DNA and promotes its chromosomal integration (a)**  
717 Transformation frequencies after electroporation with a chemically synthesized single-  
718 stranded DNA (75 -mer) coding for streptomycin resistance as donor DNA. Bars correspond to  
719 the average and standard deviation from at least two independent biological experiments. **(b)**  
720 Selective affinity of ComF for single-stranded DNA. Indicated concentrations of His<sub>6</sub>-ComFC  
721 were incubated with Cy5 labelled single- or double-stranded DNA substrate. The  
722 nucleoprotein complexes were resolved by native-PAGE.

723  
724 **Fig. 5: *H. pylori* ComF harbours a PRT and Zn-finger domains. (a)** Crystal structure of the  
725  $\alpha$ Rep-HpComF domain-swapped dimer. The two protein fusions are in green and blue. The  
726  $\alpha$ Rep was evolved against ComF to develop a specific interaction surface. In the crystal  
727 packing, each  $\alpha$ Rep returned to the ComF of another fusion, allowing the crystallization of an  
728 artificial dimer. The PRPP co-crystallized with the protein is in sticks, and the Zn<sup>2+</sup> ion is  
729 schematized by a sphere. **(b)** Bacterial two-hybrid assay of *H. pylori* ComF and its N-terminal  
730 and C-terminal domains. Representative images of reporter cells grown on plates  
731 supplemented with IPTG and X-Gal are shown. **(c)** Structure of ComF. The three loops  
732 characteristic of the PRTase fold are in green and the “hood” domain is in grey. The PRPP is in  
733 red sticks and the Zn<sup>2+</sup> and Mg<sup>2+</sup> ions are schematised by blue and orange spheres,  
734 respectively.

735  
736 **Fig. 6: ComF binds to nucleotides through its PRTase motif.** Thermal denaturation curves  
737 displaying melting temperature of **(a)** ComF and, **(b)** ComF-T165A with or without Adenosine  
738 monophosphate. **(c)** Single-stranded DNA binding by ComF-T165A.

#### 739 740 **Acknowledgements**

741 We thank the beamline staff for assistance and advice during data collections at Synchrotron  
742 SOLEIL (Saint-Aubin, France; beamline Proxima 2). We thank Christopher Corbinais and  
743 Mariano Prado-Acosta for the construction of the initial *comF* mutants. This work has  
744 benefited from the I2BC Macromolecular interactions measurements and Crystallization  
745 Platforms. Financial support for this work was provided by the Indo-French Centre for  
746 Promotion of Advanced research (CEFIPRA) grant 5203-5 (JPR, PPD), Agence Nationale de la  
747 Recherche grant ANR-19-CE12-0003-01 (JPR), French Infrastructure for Integrated Structural



748 Biology (FRISBI) grant ANR-10-INSB-05-01 (SQC, RG), Région Ile de France grant DIM1Health  
749 (JPR, PPD), Commissariat à l’Energie Atomique (JPR, AMDG, XV, JD), Centre National de la  
750 Recherche Scientifique (SQC, SM), *Enhanced Eurotalents* fellowship programme (CEA/EU)  
751 (PPD) and Collectivité Régionale de Martinique (LC)

752

753 **Author contributions**

754 Conceptualisation: SQC, JPR, PPD

755 Methodology: SQC, SM, PPD, AMDG, XV, JPR

756 Formal analysis: HW, JV, RG, SQC, JPR

757 Investigation: PPD, LC, SK, AMDG, SM, JD, XV, SQC, PL

758 Data curation: LC, HW, PL

759 Writing - Original Draft: PPD, SQC, JPR

760 Writing – Review and Editing: PPD, SQC, JPR. All authors read and approved the manuscript.

761 Visualisation: PPD, SK, AMDG, SM, HW, SQC, JPR

762 Supervision: JPR, SQC

763 Project administration: JPR

764 Funding acquisition: JPR, SQC

765

766 **Competing interests:** The authors declare that they have no competing interests.

767

768

<b>Table 1. Data Collection and Structure Refinement Statistics</b>		769
<b>Data collection</b>	<b>PRPP-bound B2-HpComF</b> ‡	
Space group	<i>P</i> 1	
Unit cell parameters	<i>a</i> =58Å <i>b</i> =88Å <i>c</i> =123Å <i>α</i> =80° <i>β</i> =76° <i>γ</i> =76°	
Wavelength (Å)	0.979	
Resolution range (Å)†	46.5-2.5 (2.6-2.5)	
<i>Before STARANISO</i>		
Measured/Unique reflections †	895493/77488 (57841/5398)	
Completeness (%)†	98.4 (92.6)	
Anomalous completeness (%)†	95.0 (84.8)	
<i>I</i> / <i>σ</i> ( <i>I</i> )†	15.7 (0.6)	
<i>After STARANISO</i>		
Measured/Unique reflections †	752919/63154 (44297/3158)	
Completeness (%)†	93.5 (94.2)	
Anomalous completeness (%)†	90.6 (92.7)	
<i>I</i> / <i>σ</i> ( <i>I</i> )†	19.2 (1.6)	
Redundancy †	11.9 (14.0)	
Anomalous redundancy †	6.1 (7.1)	
CC <sub>1/2</sub> †	0.999 (0.387)	
CC <sub>ano</sub> †	0.715 (0.403)	
<i>DANO</i>  / <i>σ</i> ( <i>DANO</i> )	1.404 (0.814)	
<i>R</i> <sub>merge</sub> (%)†	8.8 (140.1)	
<i>R</i> <sub>pim</sub> (%)†	2.7 (38.3)	
<b>SAD phasing</b>		
Number of sites	12	
Overall FOM	0.39	
<b>Refinement</b>		
Resolution range (Å)†	46.5-2.5 (2.6-2.5)	
Number of work/test reflections	63118/3156	
<i>R</i> / <i>R</i> <sub>free</sub> (%)†	22.1/24.5 (25.6/27.2)	
<b>Geometry statistics</b>		
Number of atoms		
Protein	12672	
Ligand/ion	184	
Water	282	
r.m.s. deviations from ideal values		
Bond lengths (Å)	0.007	
Bond angles (°)	0.87	
Average B-factor (Å <sup>2</sup> )		
From atoms	69.74	
From Wilson plot	79.46	
<b>Ramachandran plot</b>		
Favoured (%)	97	
Allowed (%)	3	
Outliers (%)	0	

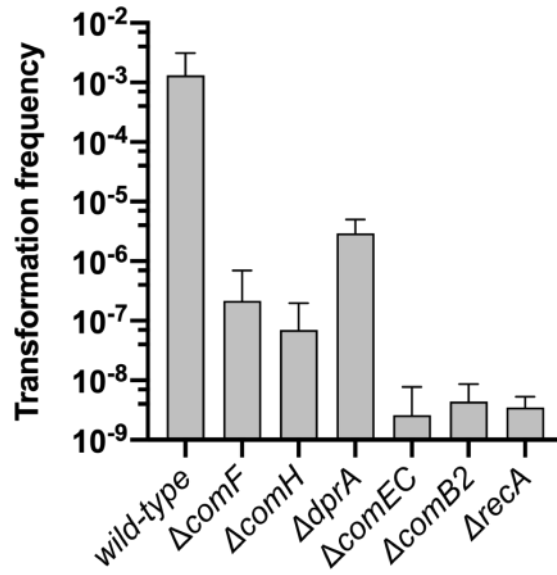
770 † Values in parentheses refer to the highest resolution shell.

771 ‡ Four merged diffraction datasets collected from one crystal, which diffracted anisotropically to 2.8  
772 Å along  $0.864 a^* - 0.025 b^* + 0.503 c^*$ , 2.7 Å along  $0.168 a^* + 0.983 b^* + 0.067 c^*$  and 2.3 Å along -  
773  $0.018 a^* + 0.097 b^* + 0.995 c^*$ .

774

**a**

Figure 1



**b**

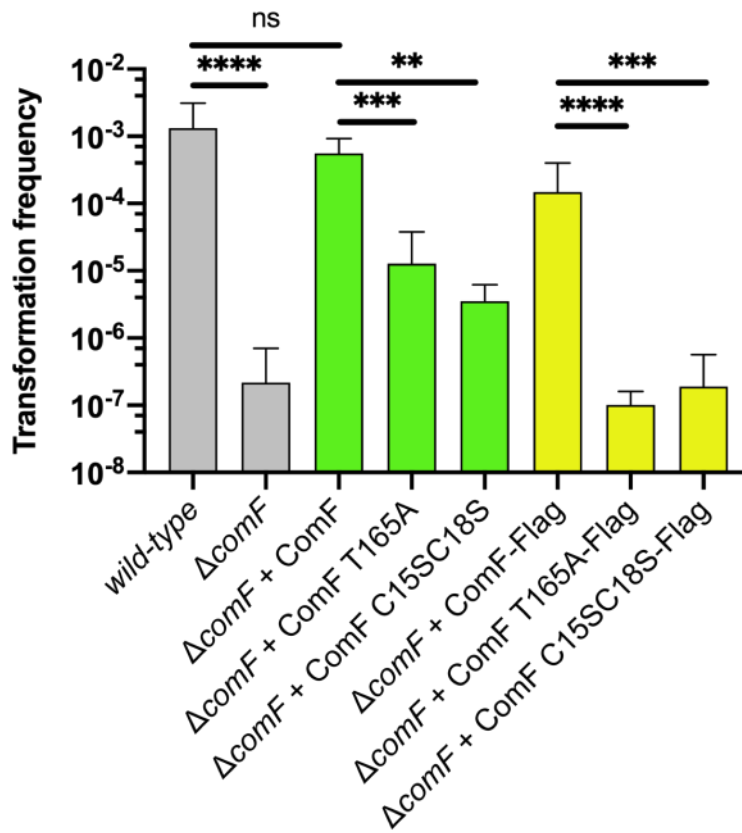


Figure 2

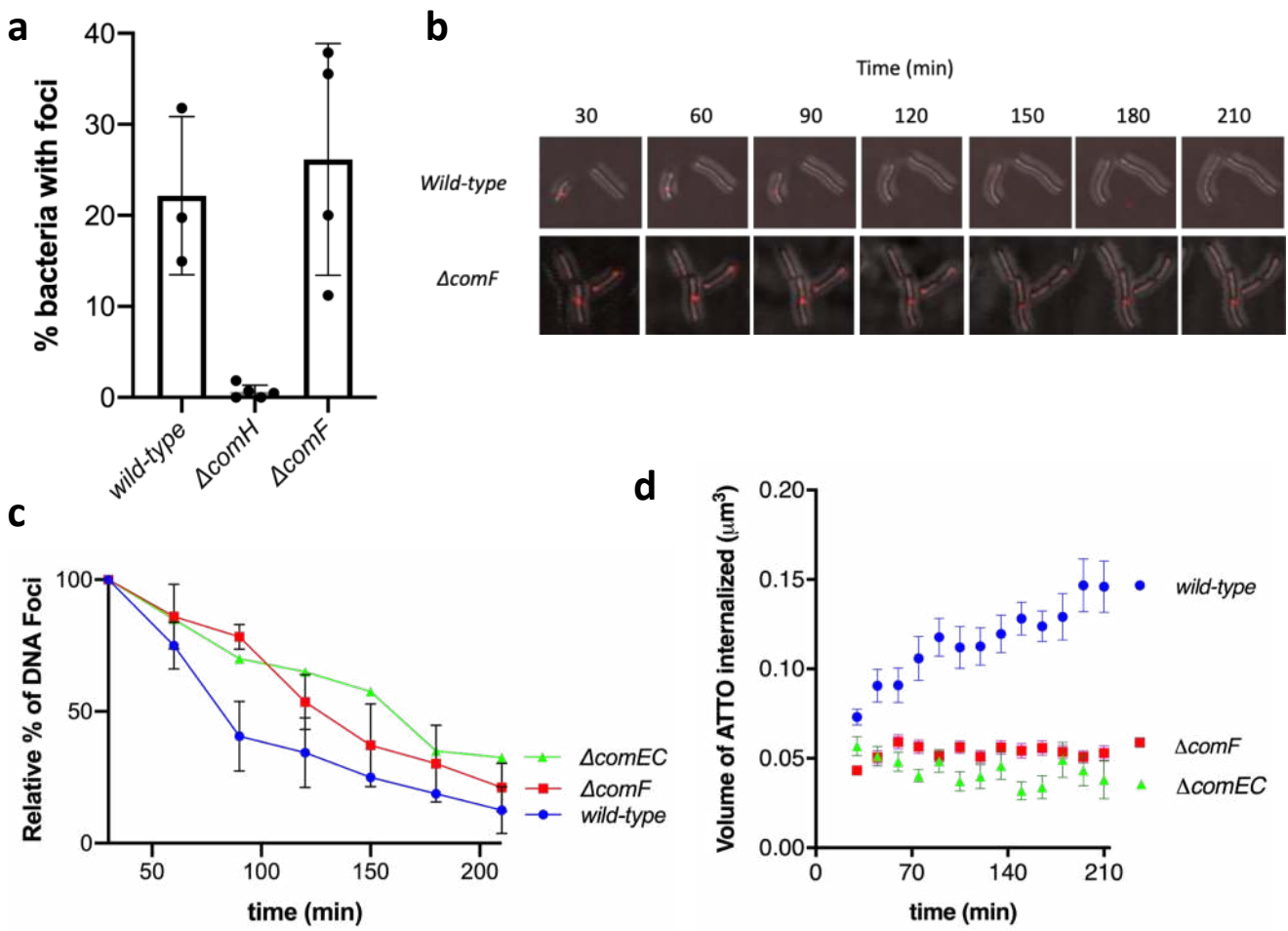


Figure 3

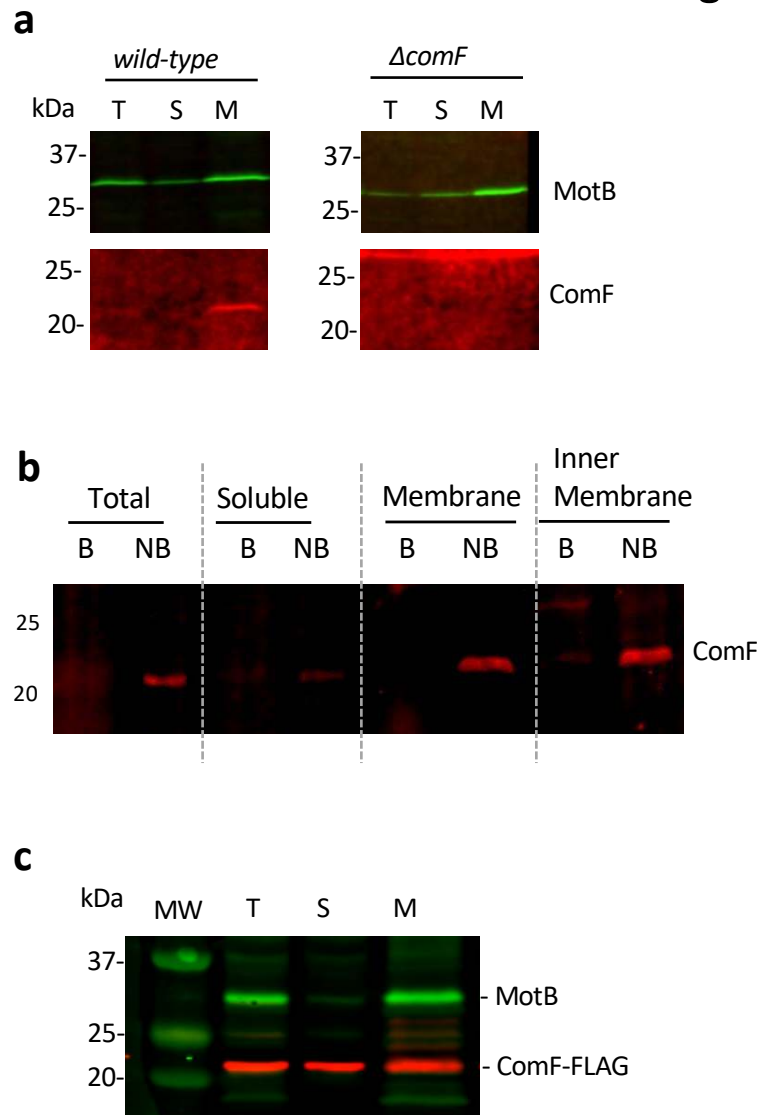


Figure 4

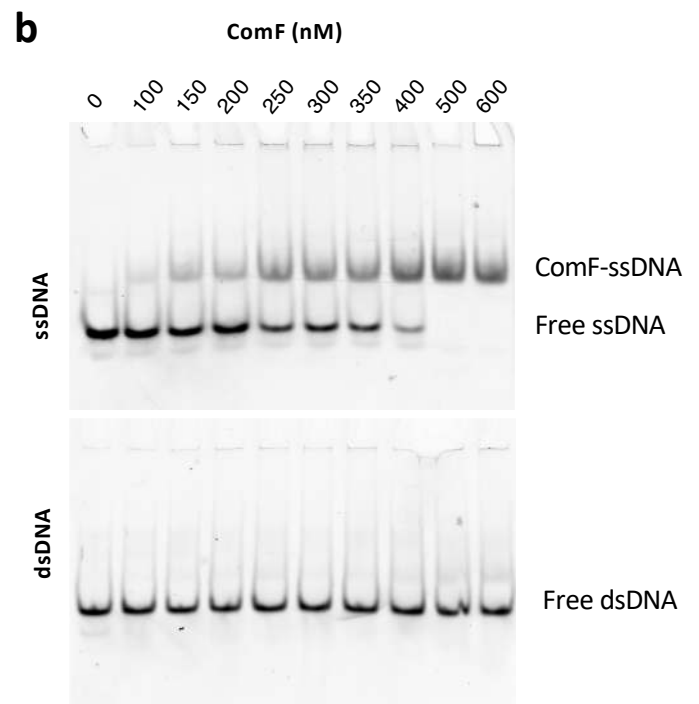
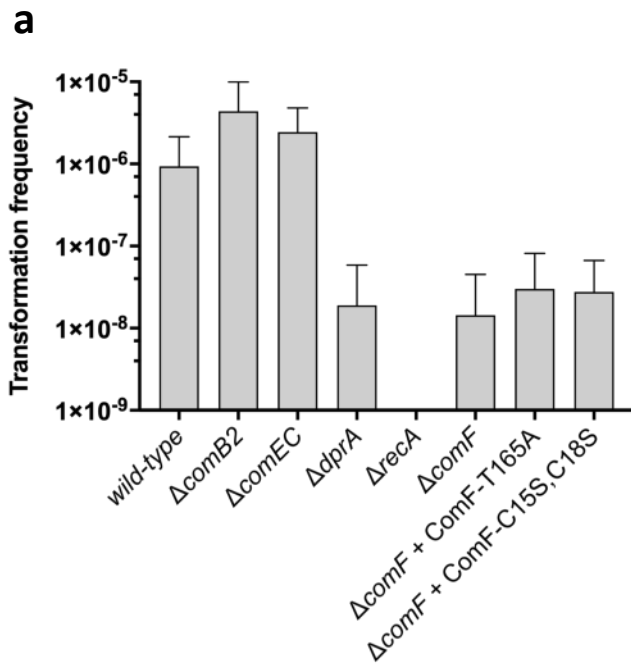


Figure 5

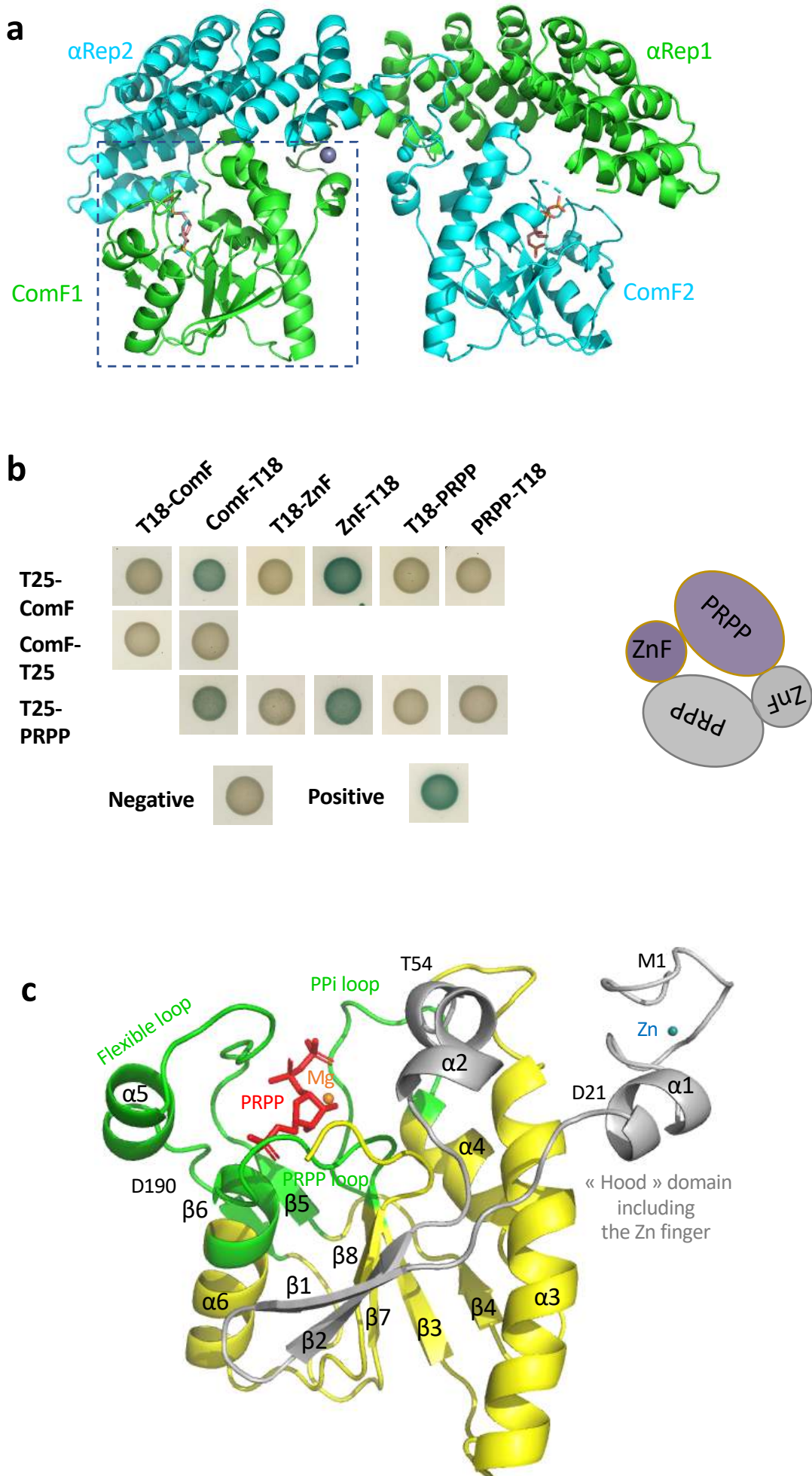


Figure 6

